known exponent.[20] If one sets $\alpha = -0.6$, $\nu = 1.3$, $\gamma = 2.3$, and $\eta = 0.23$, all of which values are within the error ranges presently obtained, then the various scaling relations, $\alpha = 2 - d\nu$ and $\alpha + 2\beta + \gamma = 2$, are satisfied. Hence these values represent the most reasonable estimates we can make at present. It is interesting that η appears to depend only weakly (if at all) on s.

The numerical results of the various approaches are not yet consistent, probably because the RG methods have not yet been sufficiently refined. However, other finite-cluster RG schemes[21] are being investigated and will no doubt lead to improved accuracy.

The authors would like to thank Dr. S. Kirkpatrick for providing them with the data of Dean and Bird.

---

*Work supported in part by the U. S. Office of Naval Research and by the National Science Foundation.

[1]K. G. Wilson, Phys. Rev. B **4**, 3174 (1971).

[2]K. G. Wilson and M. E. Fisher, Phys. Rev. Lett. **28**, 240 (1972).

[3]For a review see V. K. S. Shante and S. Kirkpatrick, Advan. Phys. **20**, 325 (1971).

[4]P. W. Kasteleyn and C. M. Fortuin, J. Phys. Soc. Jpn., Suppl. **26**, 11 (1969); C. M. Fortuin and P. W. Kasteleyn, Physica (Utrecht) **57**, 536 (1972).

[5]J. W. Essam and K. M. Gwilym, J. Phys. C: Solid State Phys. **4**, L228 (1971).

[6]J. P. Straley and M. E. Fisher, J. Phys. A: Gen. Phys. **6**, 1310 (1973).

[7]T. Kihara, Y. Midzuno, and T. Shizume, J. Phys. Soc. Jpn. **9**, 681 (1954).

[8]M. F. Sykes and J. W. Essam, Phys. Rev. Lett. **10**, 3 (1963).

[9]P. Dean and N. F. Bird, National Physical Laboratory Report No. Ma61, 1966 (unpublished).

[10]M. F. Sykes, J. L. Martin, and J. W. Essam, J. Phys. A: Gen. Phys. **6**, 1306 (1973).

[11]W. G. Rudd and H. L. Frisch, Phys. Rev. B **2**, 162 (1970).

[12]T. Niemeyer and J. M. J. Van Leeuwen, Physica (Utrecht) **71**, 17 (1974).

[13]P. G. de Gennes, Mol. Cryst. Liquid Cryst. **12**, 193 (1971); L. Mittag and M. J. Stephan, J. Phys. A: Gen. Phys. **7**, L109 (1974).

[14]M. E. Fisher and J. W. Essam, J. Math. Phys. (N. Y.) **2**, 609 (1961).

[15]G. Toulouse, to be published.

[16]R. G. Priest and T. C. Lubensky, to be published.

[17]G. R. Golner, Phys. Rev. B **8**, 3419 (1973).

[18]D. J. Wallace, J. Phys. C: Solid State Phys. **6**, 1390 (1973); A. Aharony, Phys. Rev. B **8**, 4270 (1973).

[19]R. J. Baxter, J. Phys. C: Solid State Phys. **6**, L445 (1973).

[20]Recently M. F. Sykes, M. Glen, and D. S. Gaunt, J. Phys. A: Gen. Phys. **7**, L105 (1974), found $\beta = 0.14 \pm 0.03$ by a Padé analysis of $P(q)$.

[21]L. P. Kadanoff, Phys. Rev. Lett. **34**, 1005 (1975).

Search for Gravitational Radiation at 145 Hz*

Hiromasa Hirakawa and Kazumichi Narihara†
Department of Physics, University of Tokyo, Bunkyo, Tokyo 113, Japan
(Received 19 May 1975)

We present the results of gravitational radiation experiments with two 1400-kg antennas at $\nu_0 = 145$ Hz. The square antennas, $1.65 \times 1.65 \times 0.19$ m^3, $Q_M \simeq 2.0 \times 10^5$, with electrostatic transducers of $\beta \simeq 1.8 \times 10^{-3}$, have mean effective noise energy $\overline{D} \simeq 0.034 kT_r$. The observed cross correlation of the outputs of the two detectors gives an upper limit for the relation between the mean energy spectrum density $F(\nu_0)$ and the daily occurrence rate $\dot{N}_G$ of gravitational radiation pulses: $F(\nu_0)\dot{N}_G^{1/2} \lesssim (3.6^{+1.0}_{-1.4}) \times 10^6$ J m^{-2} Hz^{-1} day$^{-1/2}$.

Large energy fluxes of gravitational radiation (GR) observed by Weber[1] at 1660 Hz have not yet been confirmed.[2] Search for GR in other frequency regions should help settle the issue and determine the GR spectrum distribution, if any. We report here the results of the correlation measurement on GR performed with two 1400-kg antennas[3] at 145 Hz.

The square antennas, $1.65 \times 1.65 \times 0.19$ m^3 with a cut on each side (Fig. 1), are fabricated from aluminum alloy (52SR) plates. The structure has symmetry D_{4h}. The fundamental in-plane vibra-
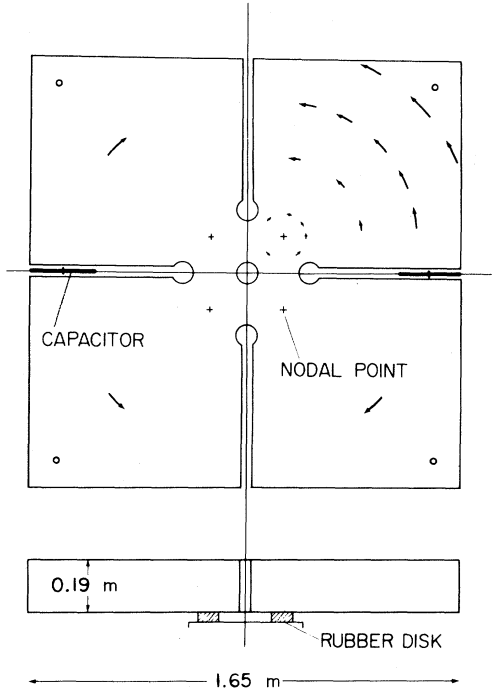
FIG. 1. Square antenna for gravitational radiation (GR) at 145 Hz. The fundamental mode of in-plane vibration B_{1g} shown here is strongly GR active. It has four nodal points which are the centers of local rotational motions. The antenna is supported at the nodal points by rubber disks. Two identical antennas were used for the correlation measurement.

tion mode B_{1g} of the plate at 145 Hz is GR active with the directivity pattern

$$f(\theta, \varphi) = \tfrac{5}{2} - \tfrac{5}{2}\sin^2\theta + \tfrac{5}{8}\sin^4\theta \cos^2(2\varphi), \quad (1)$$

$$\int f(\theta, \varphi)\,d\Omega = 4\pi, \quad (2)$$

shown in Fig. 2(a). The pattern has two peaks, $\theta = 0°$ and $180°$, of gain 4 dB over an isotropic radiator. When a short pulse of unpolarized GR hits a high-Q antenna of frequency ν ($= \omega/2\pi$) at 0 K, the energy absorbed by the antenna is[4]

$$D_G = (\pi^3 G/5c^3)M\nu^2 A_G f(\theta, \varphi)F(\nu). \quad (3)$$

$F(\nu)$ is the energy spectrum density at frequency ν in all polarizations (in units of joules per square meter per hertz) of a single GR pulse. G is Newton's gravitational constant 6.67×10^{-11} N m^2 kg^{-2}, and M is the antenna mass. The effective area A_G of an antenna is defined for each vibration mode in terms of the dynamic part of the mass quadrupole tensor $Q_{\alpha\beta} = \int \rho(x_\alpha x_\beta - \tfrac{1}{3}\delta_{\alpha\beta}r^2)$
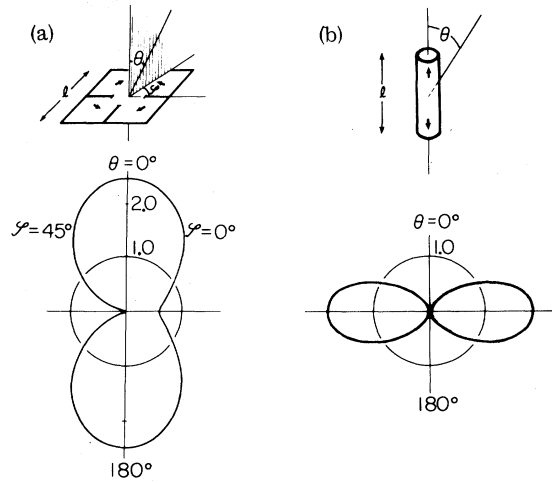

FIG. 2. Two types of GR antennas and their directivity patterns $f(\theta, \varphi)$. (a) Square antenna working in B_{1g} mode. (b) Cylindrical antenna working in $\Sigma_g{}^+$ mode.

$\times dV$ and the kinetic energy T of the vibration:

$$A_G = \frac{\sum |d^3Q_{\alpha\beta}/dt^3|^2}{TM\omega^4}. \quad (4)$$

For our antenna, A_G is $0.28l^2 \simeq 0.77$ m^2. For Weber's cylindrical antenna, with symmetry $D_{\infty h}$ and mode $\Sigma_g{}^+$, the directivity pattern is

$$f(\theta, \varphi) = \tfrac{15}{8}\sin^4\theta, \quad (5)$$

as shown in Fig. 2(b), and A_G is $(128/3\pi^4)l^2$ if contributions of radial motion to $Q_{\alpha\beta}$ and T are neglected.

Four rubber disks under four nodal points of the mode support the antenna in a horizontal position. The support yields a negligible (unloaded $Q_M \simeq 2.0 \times 10^5$) and a minimal amount of coupling to external vibrations. The rubber disks rest on an aluminum plate 20 mm thick. This plate is supported on a 300-kg steel block, which is a part of a multistage vibration-isolation system including pneumatic spring mounts of the vacuum tank housing the antenna. The estimated transmissibility from the ground to the antenna is -220 dB at 145 Hz. The oscillation of the antenna in the working mode is sensed by two electrostatic transducers, each consisting of capacitor plates, 24×7.5 cm^2, separation $x \simeq 40$ μm ($C_0 \simeq 4000$ pF), with dc potential 300 V. They are mounted inside the two opposite cuts of the antenna and electrically connected in phase. The electromechanical coupling coefficient β of the system is $\simeq 1.8 \times 10^{-3}$, as described later. The

331

audio-frequency voltage developed across a 200-MΩ resistor is fed to a field-effect-transitor amplifier with the equivalent noise resistance 350 Ω at 145 Hz. After amplification by more than 140 dB within a 15-Hz bandwidth the signal is detected by two phase-sensitive detectors with reference voltages in quadrature. The dc outputs X_i and Y_i ($i = 1, 2$) of the ith antenna, emerging

$$D_i(t) = |X_i(t) - X_i(t-1)|^2 + |Y_i(t) - Y_i(t-1)|^2 .$$

$E_i(t)$ and $D_i(t)$ contain wide-band noises from the transducer and the amplifier. If it were not for the degradation of the signal due to these noises and the bandwidth limitations, $E_i(t)$ and $D_i(t)$ should represent the oscillation energy of the antenna at t, and a hypothetical amount of energy received between $t-1$ and t if the force F_i started to work on the antenna at rest. F_i is, presumably, the sum of the gravitational force and the fluctuating internal force associated with the damping. The two antennas in separate vacuum tanks are located in the quadrangle of the Physics building at the University of Tokyo (36°N). Two seismometers, a magnetometer, and an array of plastic scintillation counters are used to monitor the environmental background.

The calibration of the system consists of determining two numbers, the total voltage gain of

through filters with $\tau = 0.5$ sec, are converted to eleven-bit digital codes every 1 sec,[5] and are subsequently processed by an on-line computer. The computer format provides for each antenna the square of the vector amplitude,

$$E_i(t) = |X_i(t)|^2 + |Y_i(t)|^2 , \tag{6}$$

and the square of the displacement of the vector during the preceding 1-sec interval,

$$\tag{7}$$

the electronic circuit and the electromechanical coupling coefficient $\beta = (C/2)V^2/T = CE^2/\mu\omega^2$, where $C = 2C_0$ is the total capacity of the transducers, E the electric field strength, and V the signal from the antenna vibrating with the kinetic energy T. $\mu = 2T/(dx/dt)^2$ is the reduced mass of the antenna referred to the plate separation x. The coefficient β is determined by measuring Q of the electrically loaded antenna, $1/Q = 1/Q_M + \beta(RC\omega)/[1 + (RC\omega)^2]$, as a function of varying magnitude of $RC\omega$. The result, $\beta \simeq 1.8 \times 10^{-3}$, agrees with that obtained from the reduced mass estimated by numerical integration of the kinetic energy. The overall gain of the system is also checked independently by exciting the antenna with known voltage pulses across a small condenser mounted in a vacant cut on the side of the antenna.

Figure 3(a) shows the distributions of E_1 and E_2 taken over 72 h. They almost agree with a Boltzmann distribution at room temperature $T_r = 290$ K, $\overline{E}_1 \simeq \overline{E}_2 \simeq kT_r$. To go into details,[6] a normalized autocorrelation function $\xi_i(s)$ is obtained for each of the dc outputs $X_i(t)$. $\xi_i(s)$ consists of two parts. The first term, representing the ther-
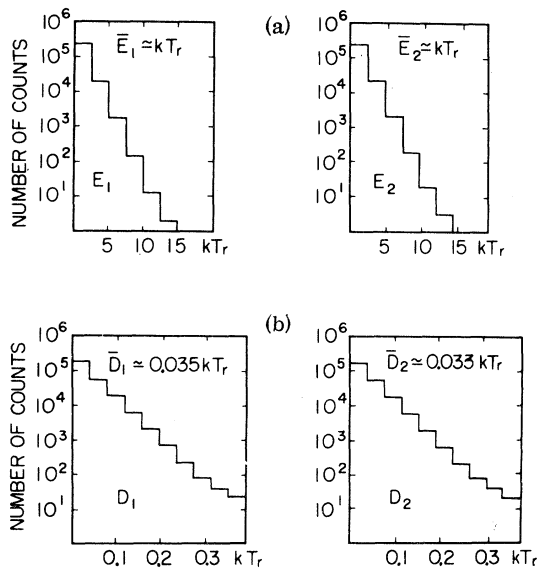

FIG. 3. Histograms showing the distributions of the size of signals from GR antennas, taken over 72 h. (a) Distributions of $E_1(t)$ and $E_2(t)$. (b) Distributions of $D_1(t)$ and $D_2(t)$.
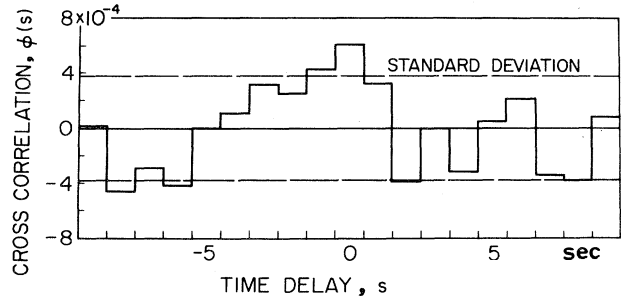

FIG. 4. Cross correlation $\phi(s)$ between signals from two GR antennas, $D_1(t)$ and $D_2(t+s)$, taken over 80 days (August–November 1974). Total number of samplings is $N_T = 6.9 \times 10^6$. Standard deviation of $\phi(s)$ is $N_T^{-1/2} = 3.8 \times 10^{-4}$.

mal vibration of the antenna at 145 Hz, shows a long-period damped oscillation due to frequency offset of the local oscillator. The second term, the noise component, decays with the time constant τ and is clearly distinguished from the first term. The size of the second terms thus determined for $\xi_1(s)$ and $\xi_2(s)$ indicates that 1.5% of E_1 and 1.2% of E_2 are wide-band noises. The distributions of D_1 and D_2 shown in Fig. 3(b) have mean values $\overline{D}_1 \simeq 0.035 kT_r$ and $\overline{D}_2 \simeq 0.033 kT_r$, which agree with calculations within 15%. No distinct correlation between D_1 and D_2 has been observed. Figure 4 shows the cross correlation of $D_1(t)$ and $D_2(t+s)$,

$$\phi(s) \equiv \frac{\langle D_1(t) D_2(t+s) \rangle_{av}}{\langle D_1(t) \rangle_{av} \langle D_2(t) \rangle_{av}} - 1, \tag{8}$$

taken over 80 days (August–November 1974), with the total number of samplings $N_T = 6.9 \times 10^6$, and the time delay s ranging from -9 to 9 sec. If an extra event of duration τ_0 ($\tau_0 \ll 1$ sec) and size D_G occurred in a time interval, in which the antenna i would have yielded $D_1{}^*$ without this event, the result is $D_1{}^* + D_G + D_{Ii}$, where D_{Ii} is the interference term. Hence N_T samplings, of which N_G ($\ll N_T$) contain an extra event apiece, yield

$$\sum D_1(t) D_2(t) = (N_T - N_G) \langle D_1{}^* D_2{}^* \rangle_{av} + N_G \langle (D_1{}^* + D_G + D_{I1})(D_2{}^* + D_G + D_{I2}) \rangle_{av}$$

$$= N_T \langle D_1{}^* \rangle \langle D_2{}^* \rangle + N_G \langle (D_1{}^* + D_2{}^*) \rangle \langle D_G \rangle + N_G \langle D_G{}^2 \rangle,$$

$$\sum D_1(t) D_2(t+s) = (N_T - 2N_G) \langle D_1{}^* D_2{}^* \rangle + N_G \langle (D_1{}^* + D_G + D_{I1}) D_2{}^* \rangle + N_G \langle D_1{}^* (D_2{}^* + D_G + D_{I2}) \rangle$$

$$= N_T \langle D_1{}^* \rangle \langle D_2{}^* \rangle + N_G \langle (D_1{}^* + D_2{}^*) \rangle \langle D_G \rangle, \quad s \neq 0, \tag{9}$$

where we have deleted the terms including D_{Ii} upon taking the average over the relative phase of inference. Thus we arrive at

$$\phi(0) = \langle D_G{}^2 \rangle N_G / \overline{D}^2 N_T, \tag{10}$$

with $\overline{D} \simeq \langle D_1{}^* \rangle \simeq \langle D_2{}^* \rangle \simeq \overline{D}_1 \simeq \overline{D}_2 \simeq 0.034 kT_r$. Actually the situation is a bit more complex because of the finite time constant τ of the filter at the output of the detectors. The response of these filters to a unit step function has a wave form $1 - \exp(-t/\tau)$. Thus an event at time t shows up not only in the term $D_i(t')$, $0 < t' - t \leqslant 1$, but also in $D_i(t'+1)$ and a few subsequent terms. A rigorous calculation, as well as experiments with simulation pulses, hence gives

$$\phi(0) = 0.27 \langle D_G{}^2 \rangle N_G / \overline{D}^2 N_T, \tag{11}$$

in place of Eq. (10) for $\tau = 0.5$ sec and the sampling interval of 1 sec.[7] Assuming an exponential distribution for D_G, we have $\langle D_G{}^2 \rangle = 2 \langle D_G \rangle^2$. Then, from the observed null-delay excess

$$\phi(0) = (6.0 \pm 3.8) \times 10^{-4}, \tag{12}$$

we obtain a relation between $\langle D_G \rangle$ and the daily occurrence rate $\dot{N}_G$ of the extra events:

$$\langle D_G \rangle \dot{N}_G{}^{1/2} = (0.33^{+0.09}_{-0.13}) kT_r \; \text{day}^{-1/2}. \tag{13}$$

According to Eq. (3) an increment $D_G = kT_r$ of the antenna energy corresponds, if it is the result of a GR event, to the mean GR energy spectrum density 1.1×10^7 J m^{-2} Hz^{-1} from isotropic sources. Therefore, Eq. (13) leads to an upper limit

$$F(\nu_0) \dot{N}_G{}^{1/2} \leqslant (3.6^{+1.0}_{-1.4}) \times 10^6 \; \text{J m}^{-2} \; \text{Hz}^{-1} \; \text{day}^{-1/2}, \tag{14}$$

for GR at $\nu_0 = 145$ Hz. An energy release of 1 solar mass $M_\odot c^2$ at a distance of 8 kiloparsecs generates an energy flux 2.3×10^5 J m^{-2}. Therefore, postulating sources at the galatic center ($\delta = -29°$) with $\langle f(\theta, \varphi) \rangle_{av} = 0.97$ averaged over the diurnal motion, we obtain a relation for the mass-energy loss from the galaxy into GR,

$$\left(\frac{\text{energy of single pulse}}{\text{pulse bandwidth}} \right)_{\text{at 145 Hz}} \dot{N}_G{}^{1/2} \leqslant (16^{+4}_{-6}) M_\odot c^2 \; \text{Hz}^{-1} \; \text{day}^{-1/2}. \tag{15}$$

Because of the factor ν^2 in Eq. (3), the cross section of a GR antenna of a given mass and effective area is $\sim 10^2$ times smaller in the 100-Hz region than in the 1000-Hz region. Thus, while the perfor-

mance of our system given in terms of the mean effective noise energy $\bar{D} \simeq 0.034kT_r$ compares favorably with the best results reported in higher-frequency bands, we have inevitably arrived at a rather large limit for the GR energy spectrum density $F(\nu_0)$ at 145 Hz given by Eq. (14).

We are grateful to Mr. Kenji Tsunemoto and Mr. Masa-Katsu Fujimoto for their contributions during various phases of the experiment. We thank Mr. Y. Kamiya and Mr. K. Tsubono for their cooperation.

---

[1] J. Weber, Phys. Rev. Lett. 22, 1320 (1969), and 24, 276 (1970), and 25, 180 (1970), and Nature (London) 240, 28 (1972); J. Weber, M. Lee, D. J. Gretz, G. Rydbeck, V. L. Trimble, and S. Steppel, Phys. Rev. Lett. 31, 779 (1973).

[2] V. B. Braginskii, A. B. Manukin, E. I. Popov, V. N. Rudenko, and A. A. Khorev, Pis'ma Zh. Eksp. Teor. Fiz. 16, 157 (1972) [JETP Lett. 16, 108 (1972)]; J. A. Tyson, Phys. Rev. Lett. 31, 326 (1973); D. Bramanti, K. Maischberger, and D. Parkinson, Lett. Nuovo Cimento 7, 665 (1973); R. W. P. Drever, J. Hough, R. Bland, and G. W. Lessnoff, Nature (London) 246, 340 (1973); J. L. Levine and R. L. Garwin, Phys. Rev. Lett. 33, 794 (1974).

[3] Details of our GR detectors will be published elsewhere.

[4] On the assumption that the resonance width ν/Q of the antenna cross section $\sigma(\theta, \varphi, \nu)$ is much smaller than the bandwidth of the incoming GR pulse spectrum $F(\nu)$, Eq. (3) is derived from $D_G = \int \sigma(\theta, \varphi, \nu) F(\nu) \, d\nu = F(\nu) \int \sigma(\theta, \varphi, \nu) \, d\nu$.

[5] These time constants were chosen so that the lowest possible temperatures are achieved for D_i.

[6] J. L. Levine and R. L. Garwin, Phys. Rev. Lett. 31, 173 (1973).

[7] In this case $\phi(-1)$ and $\phi(+1)$ have a finite magnitude, $0.11\phi(0)$.

Simple Quark-Counting Predictions for Band Structure in $p + \mathrm{Be}^9 \to (h^+ + h^- + X, \; h^+ + h^+ + X, \; h^- + h^- + X)$*

Alan Chodos and Jorge F. Willemsen

Laboratory for Nuclear Science and Department of Physics, Massachusetts Institute of Technology, Cambridge, Massachusetts 02139

(Received 16 June 1975)

A model based on simple quark counting is presented, which describes the inclusive production of charged hadron pairs at large transverse momenta. Predictions are given for the ratios of cross sections for $p + \mathrm{Be}^9 \to h_1 + h_2 + X$, where h_1 and h_2 are any of p, $\bar{p}$, π^+, π^-, K^+, and K^-. The essential feature of the model is that the valence quarks of the initial particles must be included in the counting.

Recently, preliminary data have been reported[1] on the reaction

$$p + \mathrm{Be}^9 \to h^+ + h^- + \text{anything} \tag{1}$$

at 28 GeV incident energy. Here $h^+ + h^-$ represents a pair of oppositely charged hadrons which are detected coming off at approximately 90°, back to back, in the center-of-mass system. The observed positively charged hadron is p, π^+, or K^+; the negatively charged hadron can be any of the corresponding antiparticles. Thus, in all, nine reactions have been studied.

Because the data have not been fully analyzed, only the gross features are known. These are as follows:

(i) For each reaction, the cross section $d\sigma/dM$ is observed to fall exponentially as a function of M in the region $2 \lesssim M \lesssim 5$ GeV/c^2. Here M is the invariant mass of the emitted pair. All the cross sections fall with apparently identical slopes.

(ii) Instead of nine different curves, one observes three bands with an order-of-magnitude separation between bands. The $p + \pi^-$ points form the top band. The cross sections for $\pi^+ + \pi^-$, $K^+ + \pi^-$, $p + \bar{p}$, and $p + K^-$ cluster to form the second band. The spread of this band is about a factor of 2. In the bottom band are the reactions producing $\pi^+ + K^-$, $K^+ + K^-$, $\pi^+ + \bar{p}$, and $K^+ + \bar{p}$. These are spread by a factor of perhaps $2\frac{1}{2}$ or 3.

In this Letter we present a simple model which